

Short Communication

## Removal of Cr(VI) From Electroplating Industry Effluent via Electrochemical Reduction

Shiyou Li<sup>1</sup>, Zhongqing Hu<sup>1</sup>, Shuibo Xie<sup>1,2</sup>, Haiyan Liu<sup>1</sup>, Jinxiang Liu<sup>1,\*</sup>

<sup>1</sup> Hunan Provincial Key Laboratory of Pollution Control and Resources Technology, University of South China, Hengyang, Hunan, 421001, P.R. China.

<sup>2</sup> Key Discipline Laboratory for National Defence for Biotechnology in Uranium Mining and Hydrometallurgy, University of South China, Hengyang, Hunan, 421001, P.R. China.

\*E-mail: [liu2000gps@sina.com](mailto:liu2000gps@sina.com)

Received: 6 October 2017 / Accepted: 19 November 2017 / Published: 16 December 2017

In the present work, an electrochemical reduction process with iron and titanium electrodes was investigated for hexavalent chromium (Cr(VI)) removal. The removal of Cr(VI) and its resulting species was investigated by measuring the efficiency of the electrochemical reduction treatment. For the Cr(VI) removal, a lower performance was found for the titanium electrode than the iron electrode. Therefore, the resulting Cr(VI) reduction, which occurred through electrochemical reduction using iron electrodes, was chemical reduction by the anodically generated Fe(II). Furthermore, the resulting Cr(III) was efficiently precipitated as Cr(OH)<sub>3</sub> and was rapidly removed from solution.

**Keywords:** Pollution management; Electrode configuration; Industry Effluent; Electrochemical reduction; Cr(VI) removal

### 1. INTRODUCTION

A series of environmental problems have created with the development of industry and civilization. For decades, irresponsible discharge of a large number of pollutants into the environment has been a difficult issue. Chromium ions are among these pollutants and are produced from printing inks, corrosion inhibitors, pigments, chemical catalysts, leather tanning, electroplating, and metallurgy. The toxicological and chemical performance of chromium is determined by its oxidation state: Cr(VI) or Cr(III). Cr(VI) exhibits a high mobility in the environment since it is highly soluble in water [1, 2]. Under alkaline or slightly acidic conditions, Cr(III) can easily precipitate as Cr(OH)<sub>3</sub> since it is less soluble in water [3, 4]. More importantly, Cr(VI) has been confirmed as a human carcinogen and has an inhalation toxicity to a majority of living organisms [5-7]. As a necessary nutrient for the human body, trivalent chromium is 500 to 1000 times less toxic toward living cells than hexavalent

chromium [8, 9]. However, certain adverse health effects may be caused after long periods of excessive Cr(III) exposure [10-12]. Hence, the to-be-discharged Cr-contaminated wastewater must be treated. It is worth noting that the regulated discharge Cr(VI) amount to surface water was set at <0.05 mg/L (Chinese Environmental Protection Agency (USEPA)), and the total chromium level was set at <0.1 mg/L [13-15].

The use of porous carbon felt and graphite felt as cathode materials for the electrochemical removal of chromium from wastewater has been previously reported. To effectively remove chromium from plating industry effluents, the application of bipolar iron electrodes for the electrochemical precipitation of Cr(VI) has been proposed [16, 17]. After studying the chemical reduction, electrochemical reduction and electroreduction of Cr(VI), it was found that electroreduction required 10 times more consumption of power than the electrochemical reduction [18]. Despite the high consumption of power, the decontamination of sludge by iron contributed to the recovery and reusability of water and chromium. As shown in the electrochemical precipitation, which involved the removal of Cr(VI) from ground water, an increase in the Fe(II) dosage was observed as the initial Cr(VI) concentration decreased in the feed water. The use of scrap iron in the reduction of scrap iron was also reported in a divided electrochemical cell that generated electrical energy through a galvanic cell [19, 20]. This report was novel in that it minimized the overall power consumption by storing and further using the DC energy generated during the Cr(VI) reduction for electrolysis. As shown with the relationship between the cell current and cell voltage, an increment was found in the rate of the Cr(VI) reduction and energy output as the initial concentration of Cr(VI) and the solution temperature increased. The use of continuous and batch electrochemical reactors in removing Cr(VI) from electroplating industry wastewater has been elaborately studied by Martinez and co-workers [21, 22]. The overall kinetic model was confirmed experimentally in a continuously stirred electrochemical reactor with industrial and synthetic wastewater based on a study of the Cr(VI) removal kinetics through an electrochemical reaction. This model also integrated the spontaneous dissolution of Fe(II) through corrosion in acidic media and the conversion of Fe(III) into Fe(II) through a cathodic reduction. The experimental data had a zero-order fit when the concentration of Cr(VI) was high; the fit was first-order when the concentrations were low. The current density, pH, and dispersion effects integrated in the dynamic model were reported based on the electrochemical reduction of Cr(VI) in a spiral-shaped anode – applied tubular continuous reactor [23].

In this work, two different electrodes, platinized Ti and Fe, were used to investigate the electrochemical reduction of Cr(VI) in electroplating industry wastewater. The amount of sludge formed during the process was quantified under the optimal conditions.

## 2. EXPERIMENTS

### 2.1. Preparation of Cr(VI) solutions and electroplating industry effluent

For the preparation of the Cr(VI) solutions (100 mg/L), H<sub>2</sub>SO<sub>4</sub> and NaOH were added to obtain potassium dichromate solutions with pH values of 2 and 4, and the supporting electrolytes were NaCl and Na<sub>2</sub>SO<sub>4</sub> (0.01 M). Two different electrode systems were used in this. For Fe/Fe system, both anode and cathode were made by common Fe mesh. For Fe/Ti system, Fe and Ti mesh was used for anode

and cathode, respectively. Deionized water was used throughout for the preparation of all synthetic solutions. All chemicals were analytical reagent grade. The test wastewater samples were obtained from the metal plating plant effluent, and its conductivity, pH values, and  $\text{Cl}^-$ ,  $\text{NO}_3^-$ ,  $\text{SO}_4^{2-}$ , and Cr(VI) contents are shown in Table 1.

**Table 1.** Properties of the collected electroplating industry effluent

Characteristics	Value	Characteristics	Value
Cr(VI) (mg/L)	150	Nitrate (mg/L)	0.4
Sulfates (mg/L)	124	Chlorides (mg/L)	204
pH	2.9	Conductivity (ms/cm)	24.3

### 2.2. Electrochemical reduction of Cr(VI)

A CHI 660B workstation was used for the electrochemical reduction of Cr(VI) and the corresponding characterizations. A pair of rectangular iron plates were connected to a power supply as the cathode and anode with a spacing of 1 cm. The dimensions (length  $\times$  width  $\times$  thickness) of the electrodes were 20 cm  $\times$  3 cm  $\times$  0.3 cm, and the desired effective area (20.7 cm<sup>2</sup> for the most cases) was prepared by coating part of the electrodes with insulation paint. Prior to each measurement, the electrolytes were deaerated with Ar for 20 min and then maintained under an Ar atmosphere for the duration of the measurements at room temperature (25 °C). The current density was chosen between 10 to 25 mA/cm<sup>2</sup>. Cyclic voltammetric profiles of the working electrode were recorded between 0.05 to 0.5 V at scan rate of 50 mV/s, whereas the amperometric characterizations were obtained using a solution stirred at a rate of 300 rpm with a fixed potential. Note that the determination of the Cr(VI) concentration was achieved by ICP-AES.

### 2.3. X-ray diffraction (XRD) measurement

A Siemens D500 diffractometer using Co K $\alpha$  radiation was used to record the XRD patterns for the precipitate generated by the electrochemical treatment. Prior to the measurement, the abovementioned precipitate was dried and heated in a N<sub>2</sub> flow furnace at 400 °C for 1 h and cooled to room temperature.

## 3. RESULTS AND DISCUSSION

The Fe/Fe and Fe/Ti (two anode/cathode electrodes) electrodes used for the electrolysis measurements were designed to further study the reduction mechanism of Cr(VI) using iron and titanium electrodes. Since electrochemical chromium oxidation from Cr(III) to Cr(VI) (even when the current density was 20 mA/cm<sup>2</sup>) cannot occur on the surface of the platinized titanium, it was employed as the anodic reference material [24]. Herein, the initial electrolyte pH value and initial

concentration of chromium were 7.0 and 45 mg/L, respectively. The change in the residual Cr(VI) concentration with different electrolysis times using different anode/cathode electrodes was recorded in Figure 1. The effectiveness of the iron electrodes for the removal of Cr(VI) at a concentration under 0.5 mg/L is shown in Figure 1. However, an undesirable removal was observed using the titanium electrode. Compared with the residual Cr(VI) concentration, the total chromium (Cr(VI) and Cr(III)) concentration obtained with different electrochemical reduction times was only slightly higher in the case of all the test electrodes. Rapid removal of the generated Cr(III) from solution was clearly observed via efficient precipitation as Cr(OH)<sub>3</sub>.

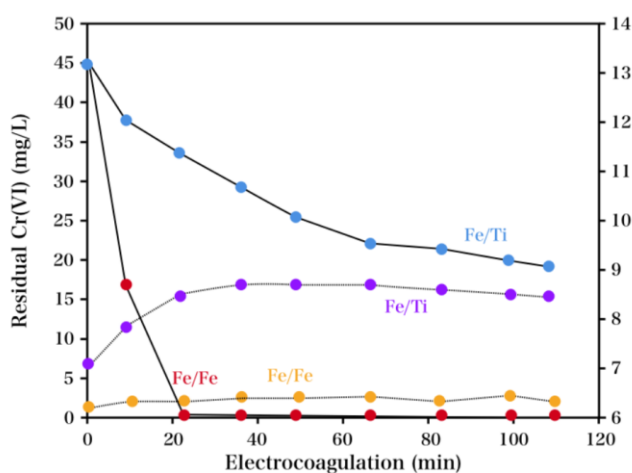


**Figure 1.** Electrochemical reduction of Cr(VI) using Fe/Fe and Fe/Ti electrodes. Electrolyte: 45 mg/L Cr(VI) + Na<sub>2</sub>SO<sub>4</sub> (1 g/L) + 100 ppm NaCl, pH = 7.0, J = 1 A/dm<sup>2</sup>.

A remarkable increase in the pH of the electrolyte was observed using the anode/cathode electrode of Fe/Fe. The hydrogen evolution at the cathode was the main factor that affected the pH change during the electrolysis. However, the concentration of chromium slightly decreased in the case of the Fe/Ti electrode. It was expected that only electro-oxidation and the reduction of water would occur during the electrolysis with iron (cathode) and platinumized titanium (anode). The chemical reduction by the anodically formed Fe(II) was confirmed to be the source of the Cr(VI) reduction through electrocoagulation with the iron electrodes.

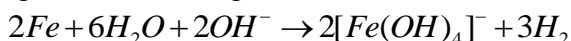
The electroreduction of Cr(VI) was investigated using different supporting electrolytes (45 mg/L), including NaNO<sub>3</sub>, NaCl, and Na<sub>2</sub>SO<sub>4</sub> (current density, 20 mA/cm<sup>2</sup>). The test specimens were collected at varying time intervals with the corresponding concentration of Cr(VI) measured. Figure 2 shows the electroreduction of Cr(VI) using varying electrolytes vs. the time. It was found that the use of NaCl decreased the Cr(VI) concentration to below 0.1 mg/L (i.e., the limit of detection (LOD)), whereas only a slight decrease was observed using NaNO<sub>3</sub> and Na<sub>2</sub>SO<sub>4</sub>. This may be due to the passivation of the electrodes since the adsorption of Cr(VI) is pH dependent, and the removal efficiency decreases with the increasing pH [25]. An impervious passive chromite film would be generated after immersing the metallic iron into a Cr(VI) solution at open circuit potentials and would influence the anodic dissolution of iron. A simple 4-probe sheets resistance measurements were

performed before and after the measurement. The results were shown in Table 1. It can be seen that the sheet resistance increased significantly after the immersing, suggesting the formation of passive chromite film. Nevertheless, passivation would be reduced in the case of the chloride ions, and their adsorption could enhance the iron dissolution [26]. When the solutions were acidic, the corrosion of iron is enhanced by nitrates, whereas only a slight influence was observed when the solutions were neutral. In comparison with the nitrates and chlorides, the sulfate ions showed less of an effect on the corrosion of iron.

**Table 1.** Sheet resistance of the electrode surface before and after immersing in different electrolytes with Cr(VI) solution.

Before	NaCl	NaNO <sub>3</sub>	Na <sub>2</sub> SO <sub>4</sub>
34.5 Ω/sq	247.4 Ω/sq	187.6 Ω/sq	54.1 Ω/sq

Regarding the amphoteric character of iron, the significant increase in the local pH at the cathode vicinity, due to hydrogen evolution, induces a “chemical” attack of iron and its hydroxide film according to the following reaction:



When treating the Cr(VI)-containing solutions, an electrochemical reduction of Cr(VI) to Cr(III) at the cathode surface was proposed to occur:



Furthermore, the hydroxyl ions that formed at the cathode increase the pH of the wastewater, thereby inducing precipitation of Cr(III) ions as the corresponding hydroxide:

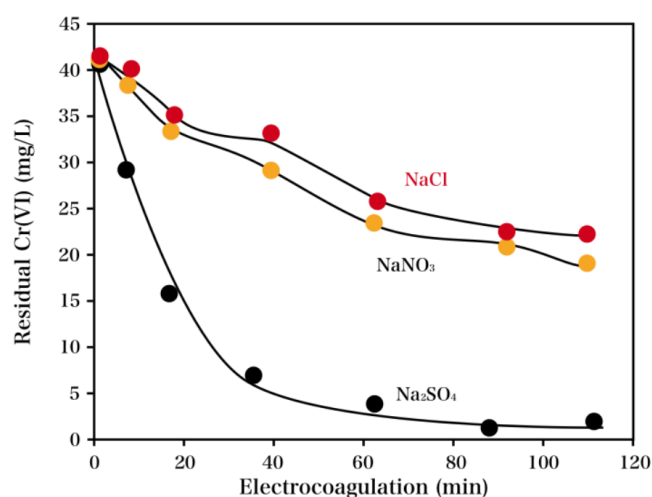
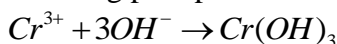


**Figure 2.** Influence of the electrolyte on the removal of Cr(VI) on a Fe/Ti electrode using the electrolyte at a fixed concentration (45 mg/L). Electrolyte: Na<sub>2</sub>SO<sub>4</sub> (1 g/L), NaSO<sub>3</sub> (1 g/L) or NaCl (1 g/L).

As shown in Figure 3, the electrochemically precipitated sludge was characterized via its XRD pattern. However, this characterization was insufficient for the sample dried at 90 °C, which is possibly due to its highly amorphous and heterogeneous structure. Therefore, the XRD pattern was further recorded after heating the sample at 400 °C for 3 h. The obtained intensities and  $d$  values of the treated sample were consistent with maghemite (JCPDS file no: 39–1346) and chromite (JCPDS file no: 04-0759). It was confirmed that dichromate was transformed into chromite after reduction and precipitation, and the remaining, unreacted iron was stabilized as maghemite at a basic pH and as magnetite at an acidic pH [27].

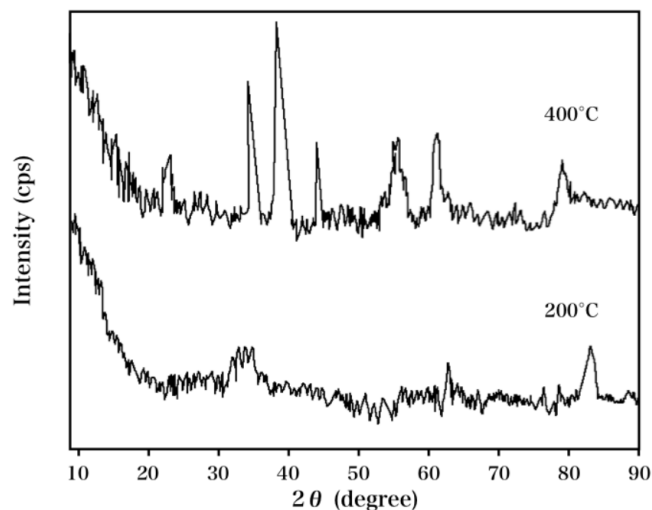


**Figure 3.** XRD patterns of the sludge after electrochemical precipitation and a heating treatment at 400 °C and 90 °C drying.

Figure 4A presents the influence of the current density on the removal of Cr(VI) over a range of 10 to 25 mA/cm<sup>2</sup>. When the current densities were high, an almost linear rate of Cr(VI) removal was observed. Furthermore, the increase in the current density doubled, which led to a faster reaction time (almost half that of the previous time) for Cr(VI) removal to levels under the LOD, which indicated that the Cr(VI) removal corresponded to Faraday's Law. It is evident that the mole ratio of Fe to Cr is approximately 1.0 at a low current density and in the initial stage of the redox reaction, which results in an increase in the current density and reaction time [28]. The pH and concentration ranges used in these experiments imply that CrO<sub>4</sub><sup>2-</sup> is the predominant form of Cr(VI) present in the medium. These results indicated the current dependent property of the reaction with higher current densities. As shown in Figure 4B, the influence of the dichromate concentration on the electrochemical removal was investigated over a range of 20 to 45 mg/L (current density, 10 mA/cm<sup>2</sup>). The necessary time for Cr(VI) removal observably increased as the initial concentration increased. For all dichromate concentrations, a linear removal rate was recorded in the initial stages, and an exponential removal rate was observed after a specific amount of time. After fitting the data to zero-order rate equations and first-order rate equations, the fit was closer to the latter.

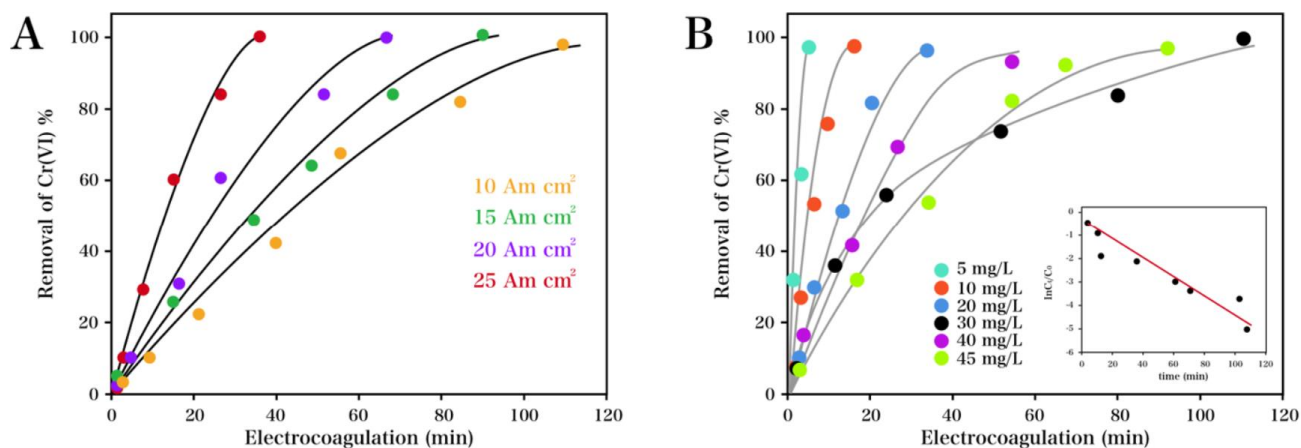


**Figure 4.** (A) Effect of the current density on Cr(VI) removal (initial concentration of 500 mg/L) at a fixed NaCl concentration of 500 mg/L. (B) Effect of the Cr(VI) concentration on the electrochemical removal at a constant current density of 10 mA/cm<sup>2</sup> and NaCl concentration of 500 mg/L.

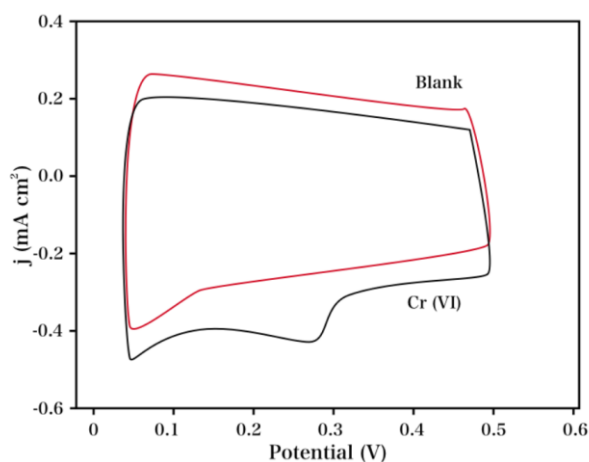


**Figure 5.** CVs obtained using an Fe/Fe configuration before and after adding Cr(VI). Electrolyte: 45 mg/L Cr(VI) + Na<sub>2</sub>SO<sub>4</sub> (1 g/L) + 100 ppm NaCl, pH = 7.0, Scan rate: 50 mV/s.

Cyclic voltammetric (CV) experiments in an acidic solution were conducted to determine the electrochemical reducing behaviour of trace levels of Cr(VI) using a Fe/Fe configuration. After the addition of Cr(VI), a relatively broad and weak peak was observed at 0.18 V (current density = 41  $\mu$ A/cm<sup>2</sup>) (Figure 5). The physical removal mechanisms explain the increase in the Cr(VI) abatement when passivation is achieved. In the same potential region of the corresponding blank CV pattern without Cr(VI), a reduction peak was not recorded, which suggested that this reduction peak resulted from the reduction of Cr(VI). Moreover, the reverse scan of the CV runs after adding Cr(VI) did not lead to a corresponding oxidation peak, which indicated the electrochemical irreversibility of this reaction. In comparison with the blank pattern, the CV pattern shifted slightly downward, which was possibly a result of the Cr(VI) reduction wave [29]. Moreover, the Ti/TiO<sub>2</sub>NT/Au configurations

exhibited an undesirable potential during further use for the removal of Cr(VI) at trace levels in spite of their distinct electrochemical performance for Cr(VI) reduction [30].

#### 4. CONCLUSIONS

This work reported the use of novel electrodes based on metallic iron and titanium to remove Cr(VI) from electroplating industry wastewater. Compared with the Fe/Ti electrode, the Fe/Fe electrode showed a much higher electrochemical reduction rate. In the case of Na<sub>2</sub>SO<sub>4</sub> as the supporting electrolyte, the trivalent chromium was removed at levels below the LOD. However, the use of NaCl as a supporting electrolyte led to a negligible reduction, and the use of NaNO<sub>3</sub> resulted in only a slight reduction. The pH increased from acidic to more basic as the Cr(VI) was removed from solution. As the current density increased, the conversion rate of chromite from Cr(VI) increased. In the case of low current densities, the Cr(VI) reduction exhibited a current control property in the initial stages, and a mass transport control property was observed as the reaction proceeded.

#### References

1. H. Xu, Z. Yang, G. Zeng, Y. Luo, J. Huang, L. Wang, P. Song and X. Mo, *Chemical Engineering Journal*, 239 (2014) 132.
2. W. Jin, Z. Zhang, G. Wu, R. Tolba and A. Chen, *RSC Advances*, 4 (2014) 27843.
3. A. Dharnaik and P. Ghosh, *Environmental technology*, 35 (2014) 2272.
4. W. Jin, H. Du, S. Zheng and Y. Zhang, *Electrochimica Acta*, 191 (2016) 1044.
5. J. Zhu, H. Gu, J. Guo, M. Chen, H. Wei, Z. Luo, H.A. Colorado, N. Yerra, D. Ding and T.C. Ho, *Journal of Materials Chemistry A*, 2 (2014) 2256.
6. H. Daraei, A. Mittal, J. Mittal and H. Kamali, *Desalination and Water Treatment*, 52 (2014) 1307.
7. H. Wang, X. Yuan, Y. Wu, X. Chen, L. Leng, H. Wang, H. Li and G. Zeng, *Chemical Engineering Journal*, 262 (2015) 597.
8. Y. Mu, Z. Ai, L. Zhang and F. Song, *ACS applied materials & interfaces*, 7 (2015) 1997.
9. X. Sun, L. Yang, Q. Li, J. Zhao, X. Li, X. Wang and H. Liu, *Chemical Engineering Journal*, 241 (2014) 175.
10. X. Guo, B. Du, Q. Wei, J. Yang, L. Hu, L. Yan and W. Xu, *Journal of hazardous materials*, 278 (2014) 211.
11. X. Yuan, Y. Wang, J. Wang, C. Zhou, Q. Tang and X. Rao, *Chemical engineering journal*, 221 (2013) 204.
12. X. Li, L. Ai and J. Jiang, *Chemical Engineering Journal*, 288 (2016) 789.
13. E. Petala, K. Dimos, A. Douvalis, T. Bakas, J. Tucek, R. Zbořil and M.A. Karakassides, *Journal of hazardous materials*, 261 (2013) 295.
14. Z. Liu, L. Chen, L. Zhang, S. Poyraz, Z. Guo, X. Zhang and J. Zhu, *Chemical Communications*, 50 (2014) 8036.
15. S. Aoudj, A. Khelifa, N. Drouiche, R. Belkada and D. Miroud, *Chemical Engineering Journal*, 267 (2015) 153.
16. M.L. Sall, A.K.D. Diaw, D. Gningue-Sall, A. Chevillot-Biraud, N. Oturan, M.A. Oturan and J.-J. Aaron, *Environmental Science and Pollution Research*, (2017) 1.
17. H. Wang, Y.-g. Liu, G.-m. Zeng, X.-j. Hu, X. Hu, T.-t. Li, H.-y. Li, Y.-q. Wang and L.-h. Jiang, *Carbohydrate polymers*, 113 (2014) 166.
18. W. Wang, J. Zhou, G. Achari, J. Yu and W. Cai, *Colloids and Surfaces A: Physicochemical and*

- Engineering Aspects*, 457 (2014) 33.
19. S.J. Fuller, I.T. Burke, D.G.G. McMillan, W. Ding and D.I. Stewart, *Water, Air, & Soil Pollution*, 226 (2015) 180.
  20. M. Bhaumik, S. Agarwal, V.K. Gupta and A. Maity, *Journal of colloid and interface science*, 470 (2016) 257.
  21. S.S. Hamdan and M.H. El-Naas, *Journal of Industrial and Engineering Chemistry*, 20 (2014) 2775.
  22. V.N. Montesinos, N. Quici, E.B. Halac, A.G. Leyva, G. Custo, S. Bengio, G. Zampieri and M.I. Litter, *Chemical Engineering Journal*, 244 (2014) 569.
  23. L. Sun, Z. Yuan, W. Gong, L. Zhang, Z. Xu, G. Su and D. Han, *Applied Surface Science*, 328 (2015) 606.
  24. R.Y. Fillit, A. Rousseau and P. Benaben, *Galvano organo traitements de surface*, (2002) 451.
  25. S. Virtanen and M. Büchler, *Corrosion science*, 45 (2003) 1405.
  26. J.-D. Kim and S.-I. Pyun, *Corrosion science*, 38 (1996) 1093.
  27. S. Musić, M. Gotić and S. Popović, *Journal of materials science*, 28 (1993) 5744.
  28. B.A. ssa, D. Therriault, E. Haddad and W. Jamroz, *Advances in Materials Science & Engineering*, 2012 (2014)
  29. W. Jin, M.S. Moats, S. Zheng, H. Du, Y. Zhang and J.D. Miller, *Electrochimica Acta*, 56 (2011) 8311.
  30. W. Jin, G. Wu and A. Chen, *Analyst*, 139 (2014) 235

© 2018 The Authors. Published by ESG ([www.electrochemsci.org](http://www.electrochemsci.org)). This article is an open access article distributed under the terms and conditions of the Creative Commons Attribution license (<http://creativecommons.org/licenses/by/4.0/>).